Supporting Information

Dual Activation Mode Containing Indanedione Based Fluorometric Probe for CN^- Sensing: Its Application in Bioimaging, Fingerprint and Food Sample Analysis

Yesudhasan Chinnaraj[a], Gouthaman Siddan[b], Velmurugan Ajithkumar[c], Perumal Varalakshmi[c], Kumar Venkatesan[d], Manickam Selvaraj[e] and Siva Ayyanar*[a]

[a]Supramolecular and Organometallic Chemistry Laboratory, School of Chemistry, Madurai Kamaraj University, Madurai-21, Tamilnadu, India.

[b]Organic Material Lab, Indian Institute of Technology-Roorkee, India.

[c]Department of Molecular Microbiology, School of Biotechnology, Madurai Kamaraj

University, Madurai-21, Tamilnadu, India.

[d]Department of Pharmaceutical Chemistry, College of Pharmacy, King Khalid University, Abha 61413, Saudi Arabia.

[e]Department of Chemistry, Faculty of Science, King Khalid University, Abha 61413, Saudi Arabia.

Corresponding author : E-mail: drasiva@gmail.com; siva.chem@mkuniversity.ac.in

1. Materials and Methods

1.1 Instrumentations

A Bruker spectrometer (400 MHz) was used to obtain the Nuclear Magnetic Resonance (NMR) spectra; chemical shift values were recorded in δ (delta) (parts per million). Electrospray Ionization Mass Spectrometry (ESI-MS) analyses were recorded in LC/Q -TOF, Agilent Instruments Limited, United States. ESI-MS was measured in positive ion mode. The collision and ionization voltage were − 70 kV and − 4.5 kV, respectively, using nitrogen as atomization and desolvation gas. The desolvation temperature was set at 300 °C. The relative amount of each part was determined from the LC-MS chromatogram using the area normalization method, which ensured a thorough analysis. The optical properties of the prepared materials were examined on a JASCO V-630 UV-vis spectrophotometer using the quartz cuvette with a 1 cm path length at 298 K. The excitation and emission slits were set to 2.5 nm for all the emission measurements. The steady-state photoluminescence (PL) emission spectra of synthesized dyes were analysed on JASCO F-8500 fluorescence spectrophotometer, Fluoromax spectrofluorometer (HORIBA) and Radical Inverted Medical Biological Microscope RTC-7.

1.2. Strock solution of PBI and anions

The PBI stock solution in DMSO was prepared at a concentration of 0.001 M to conduct naked-eye sensing and photophysical studies. The stock solutions of competitive anions CN^{-}, CO_3^{2-}, SO_3^{2-}, SO_4^{2-}, NO_2^{-}, NO_3^{-}, I^{-}, Br^{-}, $H_3PO_4^{2-}$, and SCN^{-} were made by dissolving appropriate amounts of their tetra butylammonium salts in HPLC grade water. UV-vis absorption and emission titration experiments were conducted with 20 μM probe **PBI** against 20×10^{-2} mM of various anions at 25 ^{0}C, following a thorough and well-designed experimental plan.

1.3. The determination of the detection limit

Emission spectral data of PBI confirmed the detection limits (DL) upon the gradual addition of CN^{-}.

$$\mathbf{DL = 3\,\sigma\,/S \text{ and } LOQ: 10\,\sigma\,/S}$$

where σ was the standard deviation of a blank sample, and S represented the absolute value of the slope between fluorescence intensity and CN^{-} concentration.

1.4. Job's plot and the stern-Volmer quenching efficiency.

The Job's plot method was performed as follows: A stock solution of the probe and a stock solution of tetra butyl ammonium cyanide were prepared at the same concentration in DMSO and water. The quenching efficiency can be estimated by the Stern-Volmer equation $\mathbf{F_0/F = 1 + K_{SV}[Q]}$, where $\mathbf{F_0}$ is the fluorescence intensity before the addition of anion, **F** is the fluorescence intensity after the addition of anion, and [Q] is the concentration of anion.[43]

1.5. Theoretical calculation

The molecular electrostatic potential, bond lengths, and angles were calculated using DFT. Moreover, the optimized geometries of **PBI**, **PBI-CN**, and the HOMO-LUMO energy gap for PTI and its complexes were calculated using density functional theory (DFT) with Gaussian 09 W. The DFT-based B3LYP/6-311G* model was performed for C, O, and H atoms. The molecular interaction between **PBI** and CN^- was thoroughly analysed and proposed in the DFT calculation results, ensuring a comprehensive system understanding.

1.6. Paper strip analysis

After submerging in the probe **PBI** (20 μM) solution in DMSO solvent, a Whatman paper was allowed to air dry at room temperature. A digital camera documented the colour variations on the probe **PBI** coated paper strip after further investigation with CN^-.

1.7. Latent finger print analysis

The visualization of latent fingerprints was carried out using a powder dusting technique with a fine fluorescent powder. A minimal quantity of PBI fine powder was gently applied to the target surface, ensuring uniform coverage, and allowed to adhere for approximately 5 seconds. Following this, the excess powder was carefully removed using a non-contact method to avoid frictional interaction with the latent fingerprint residue, thereby preserving its structural integrity. The developed fingerprints were then analyzed under appropriate fluorescence excitation conditions to assess the effectiveness of the visualization technique.

1.8. Bioimaging application

The fluorescence intensity of the prob **PBI** inside the cells has been assessed via the model organism Caenorhabditis elegans, a significant step in understanding this process. This simple and transparent nematode worm with a short lifecycle and a constant number of somatic cells after adulthood was the perfect candidate for this study. We followed the standard protocol for worm culture and maintenance, ensuring the reliability of results.[44] The day-1 adult worms were exposed to an S-complete medium including *E. Coli* OP50 and PBI (20 and 50 µM) in 96 well plates and allowed 2 hr in the medium at 20 ºC. The addition of CN^- (10 µM) has been done in part of the worms separated from the 96 well plates. The worms were fixed in agarose pads with or without sodium azide and anesthesia for microscopic imaging. The fluorescence imaging has been performed in an Olympus BX41 fluorescence microscope through a 450-480 exciter filter (Blue light) and emission filter 515-550 nm (Green light emission). The fluorescence images of worms were captured and adopted with an Olympus OMD camera with 8f/s without exposure, and the fluorescence intensity of each worm was analyzed via ImageJ software. Statistical analysis was performed using SPSS software and represented SEM and *p>0.05, which were considered significantly different.

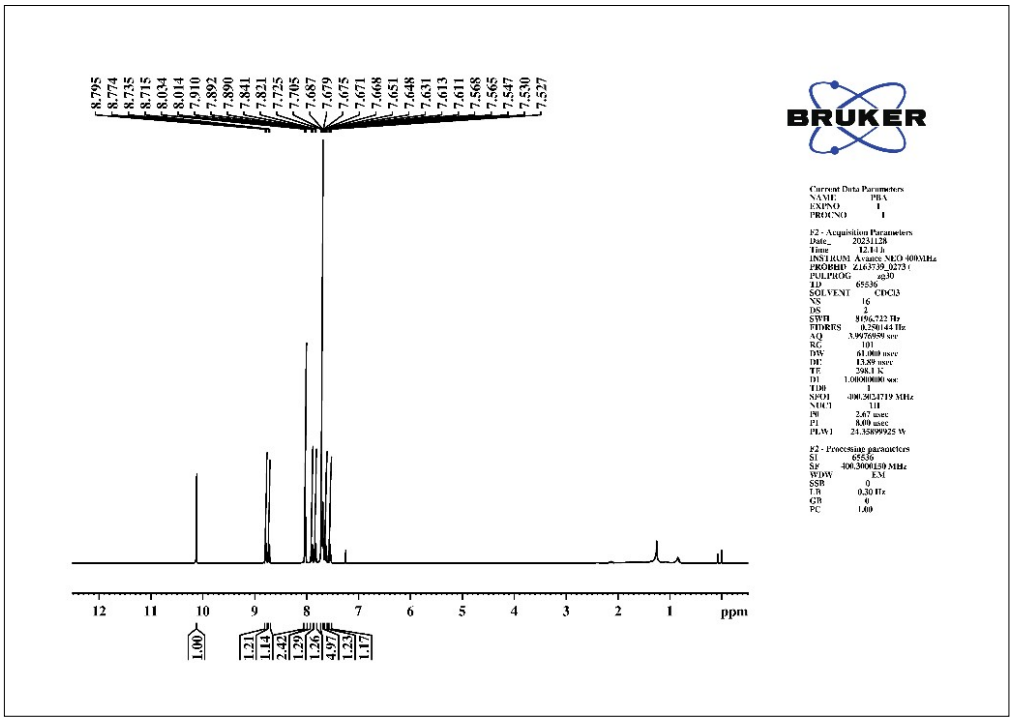

Figure: S1. ^{1}H NMR spectrum of **PBA** in $CDCl_3$

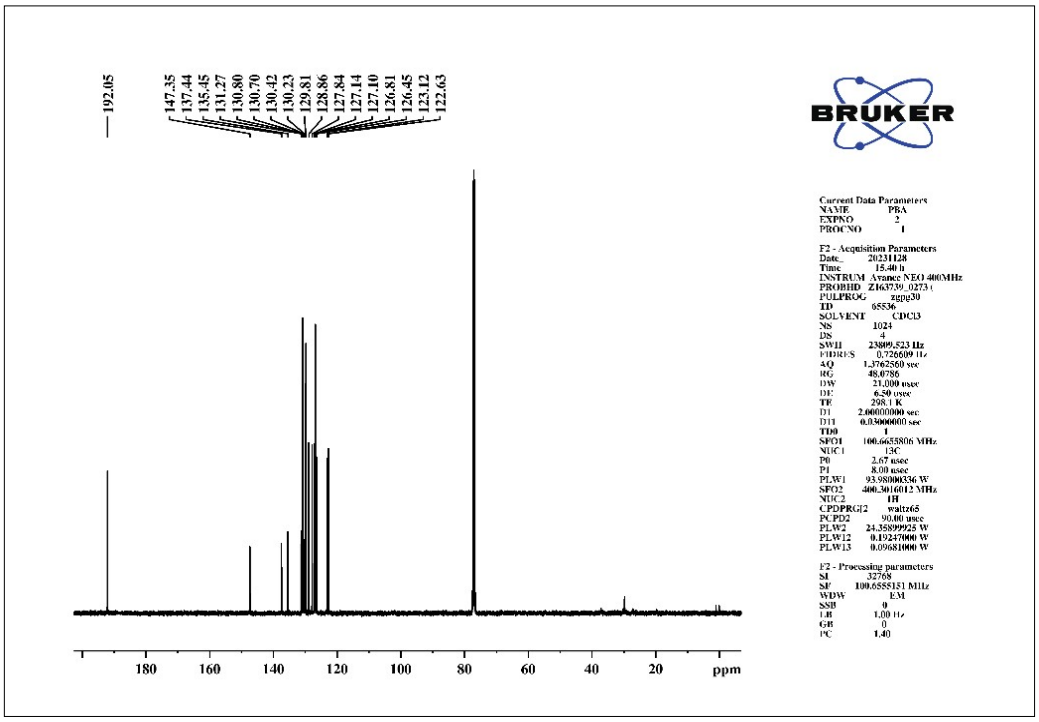

Figure: S2. **^{13}C NMR** spectrum of **PBA** in $CDCl_3$

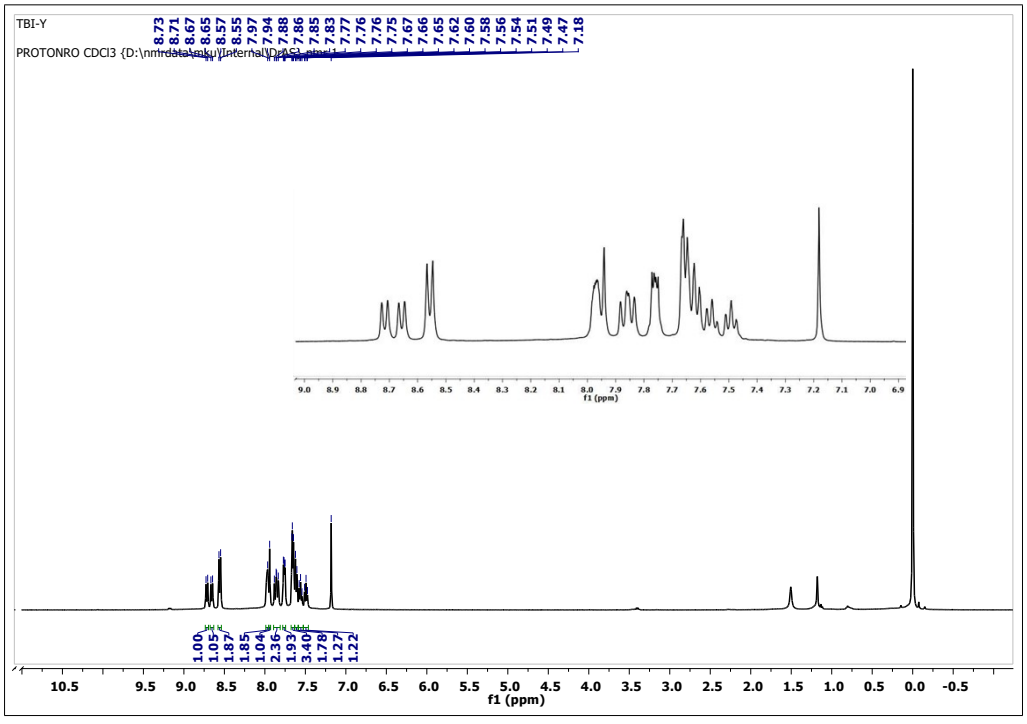

Figure: S3. **^{1}H NMR** spectrum of **PBI** in $CDCl_3$

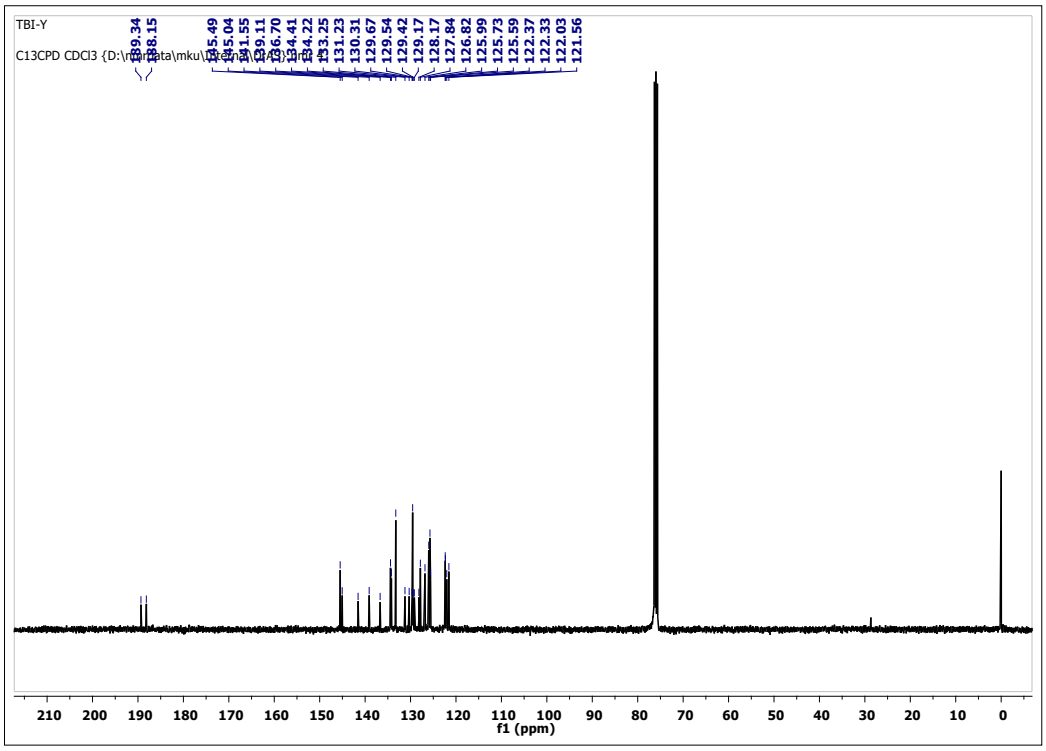

Figure: S4. **^{13}C NMR** spectrum of **PBI** in $CDCl_3$

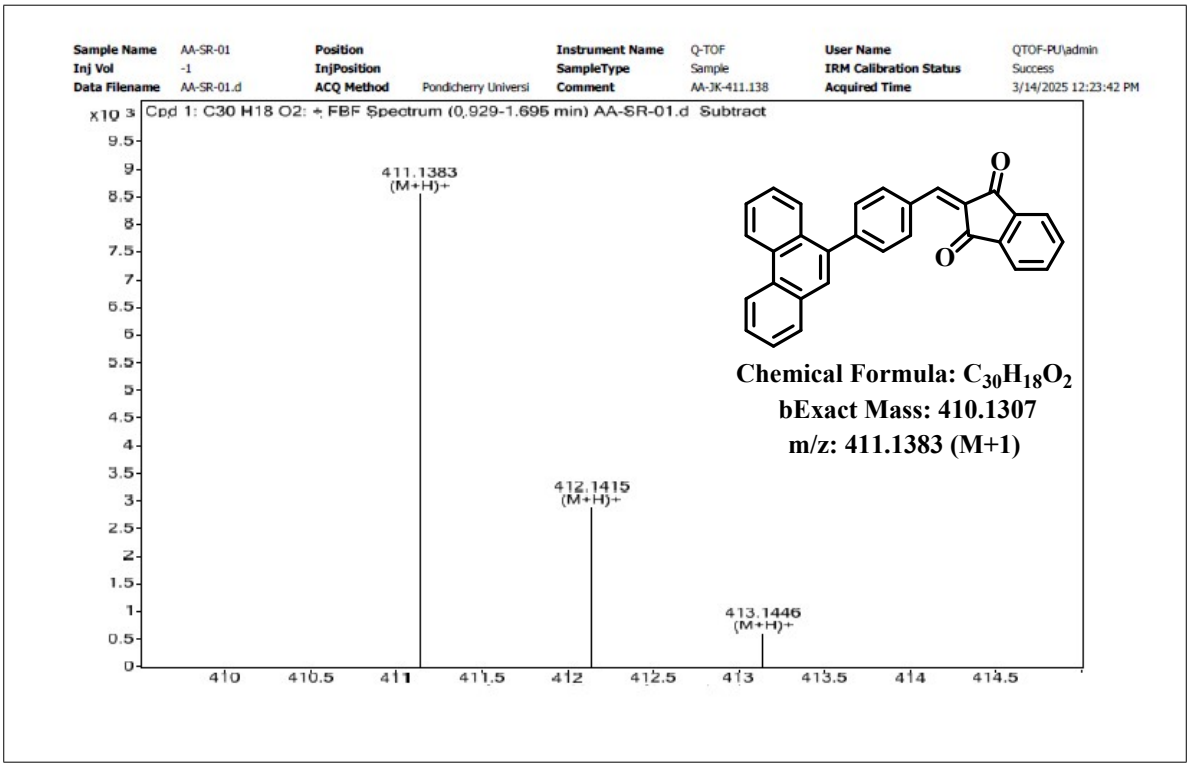

Figure: S5. HRMS spectrum of **PBI**

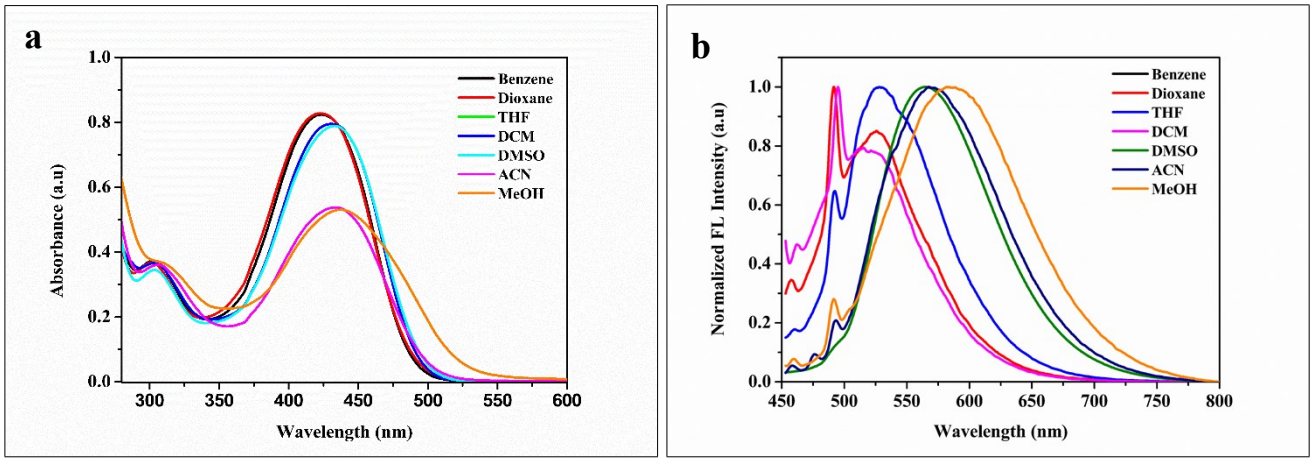

Figure: S6 a) absorption spectra of **PBI** and b) emission spectra of **PBI** with various solvents

Table: S1 Quantum yield calculation of different solvents

Entry	solvents	Quantum yield ΦS (%)
1	Benzene	8.25
2	Dioxane	8.24
3	THF	7.11
4	Dichloromethane	5.40
5	Dimethyl sulfoxide	4.08
6	Acetonitrile	3.10
7	Methanol	2.85

Table: S2 Absorption,emission and stokes shift spectral data of various solvents

Solvent	$\lambda_{ab,}$ (nm)	$\lambda_{emi,}$ (nm)	Stokes shift (cm^{-})
Benzene	422	526	4685
Dioxane	424	531	4752
THF	425	533	4767
DCM	430	543	4839
DMSO	431	567	4873
ACN	432	572	5565
MeOH	437	587	5847

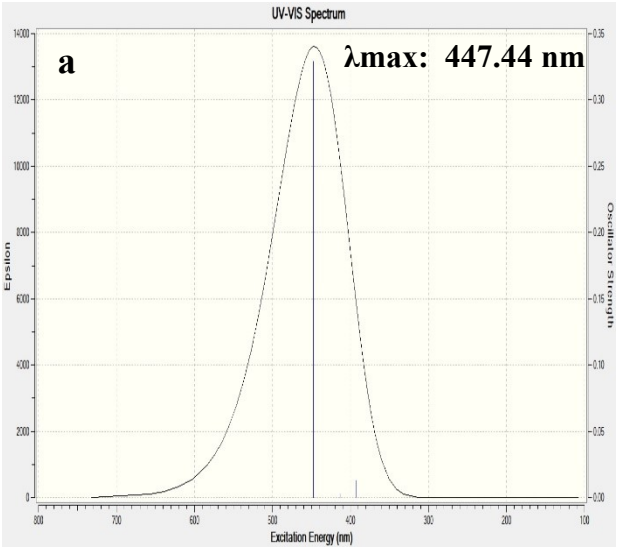
UV-VIS Spectrum
a
λmax: 447.44 nm
Epsilon
Oscillator Strength
Excitation Energy (nm)

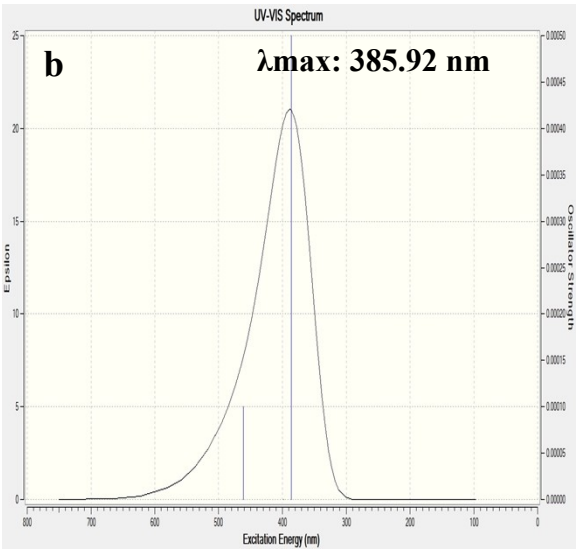
UV-VIS Spectrum
b
λmax: 385.92 nm
Epsilon
Oscillator Strength
Excitation Energy (nm)

Figure: S7. TD-DFT theoretical UV-vis spectrum of a) PBI and b) PBI-CN

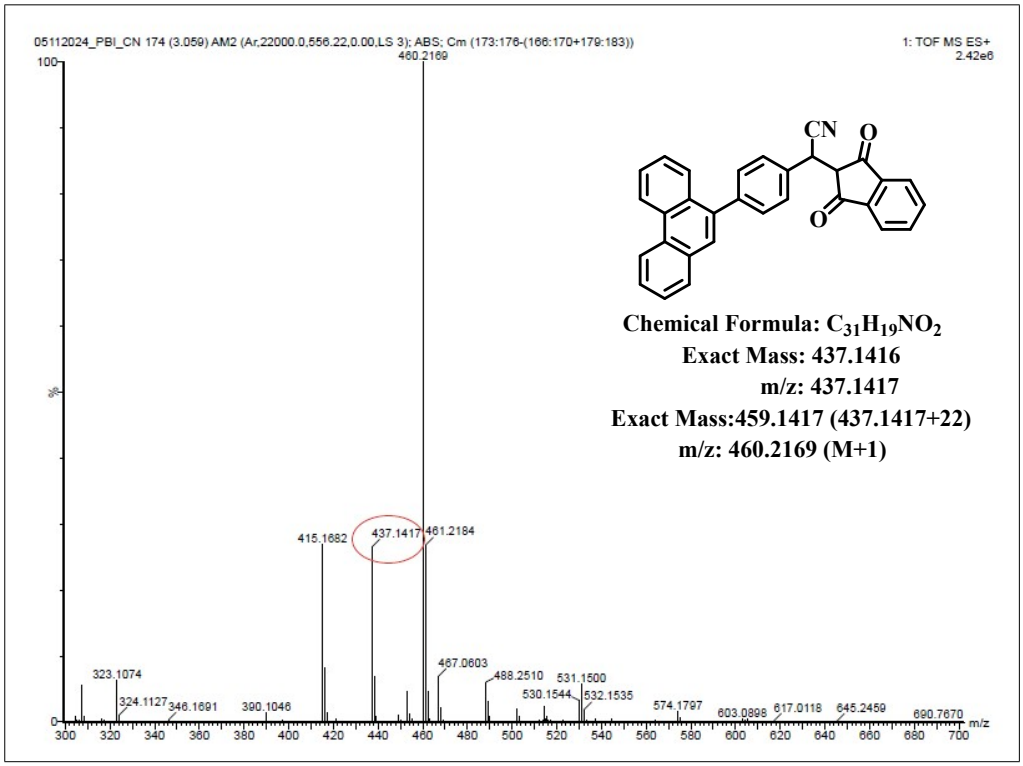

Figure: S8. HRMS spectrum of **PBI**-CN

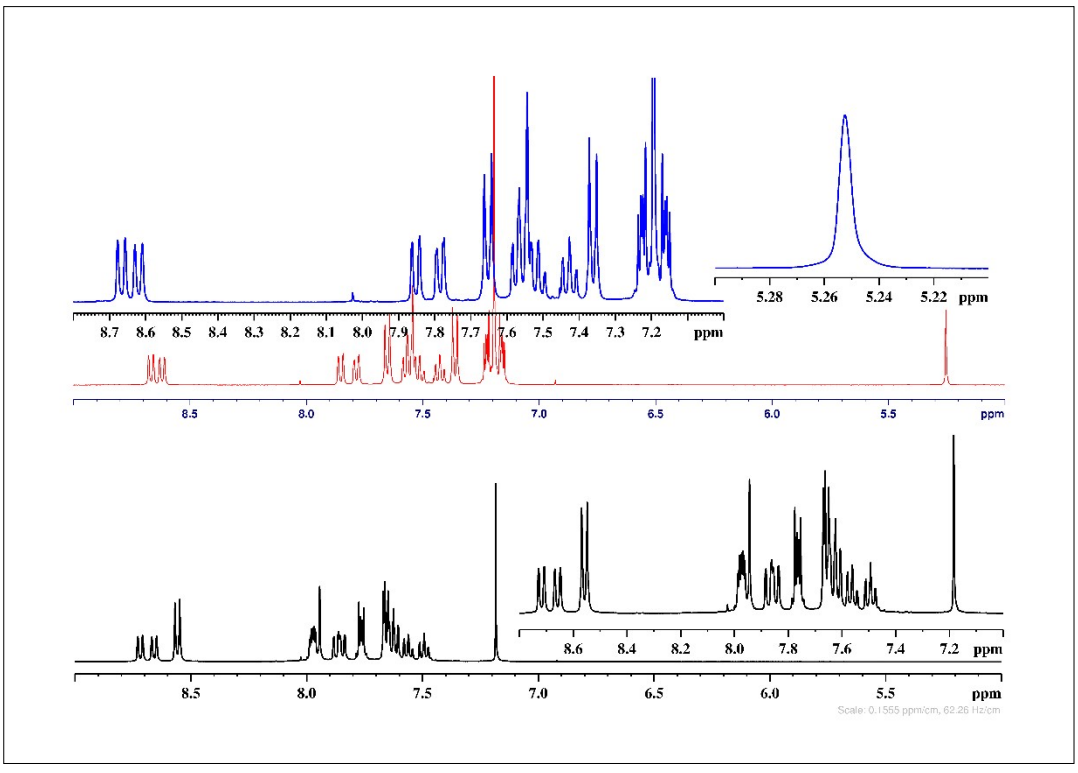

Figure S9. ^{1}H NMR Titration for PBI towards CN^{-}

Table: S3. Sensors for cyanide determination

S.NO	Sensors	LOD (M)	Reference
1	Coumarinyl-Benzothiazolyl Schiff base	0.75 µM	10
2	Bdiketone difluoroboron based	2.23 µM	13
3	Benzothiazole-phenylenediacetonitrile	0.62 µM	17
4	Indandione based	6.2×10^{-7}M	21
5	Porphyrin based	6.2×10^{-7}M	25
6	Naphthalene diimide based	4.1×10^{-7}M	28
7	Indanedione based	9.4×10^{-7}M	30
8	Present work	0.107 µM	

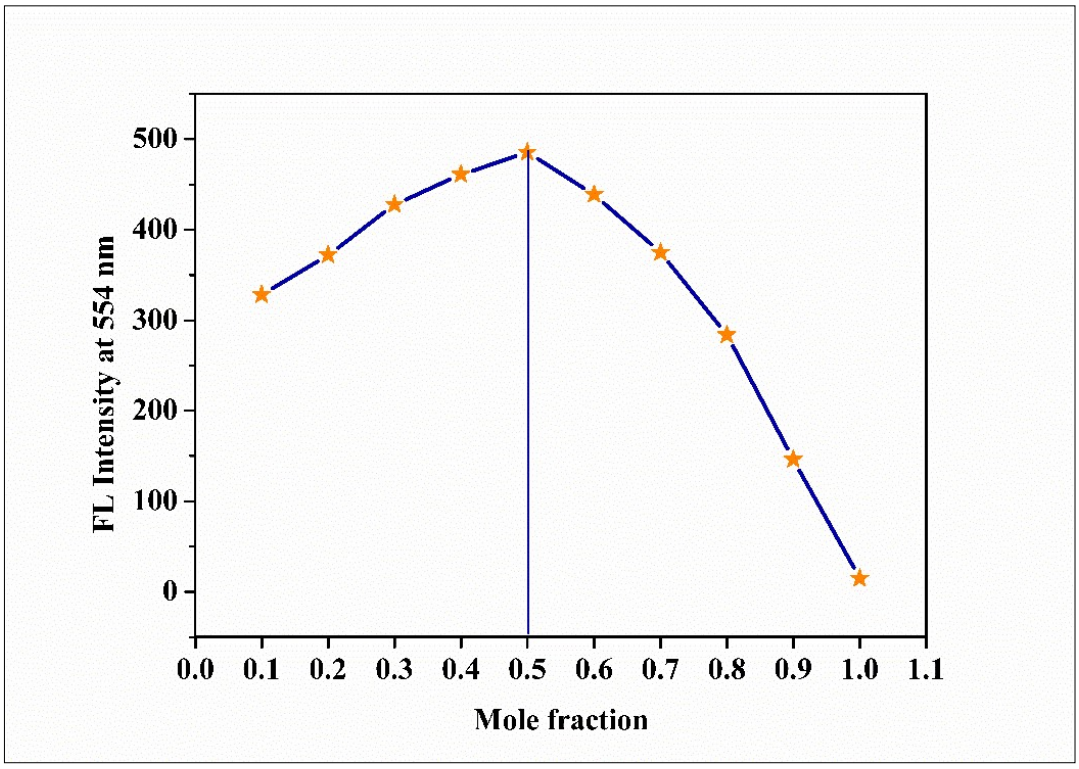

Figure S10. The Job's plot for **PBI** towards CN^{-} in the DMSO solution

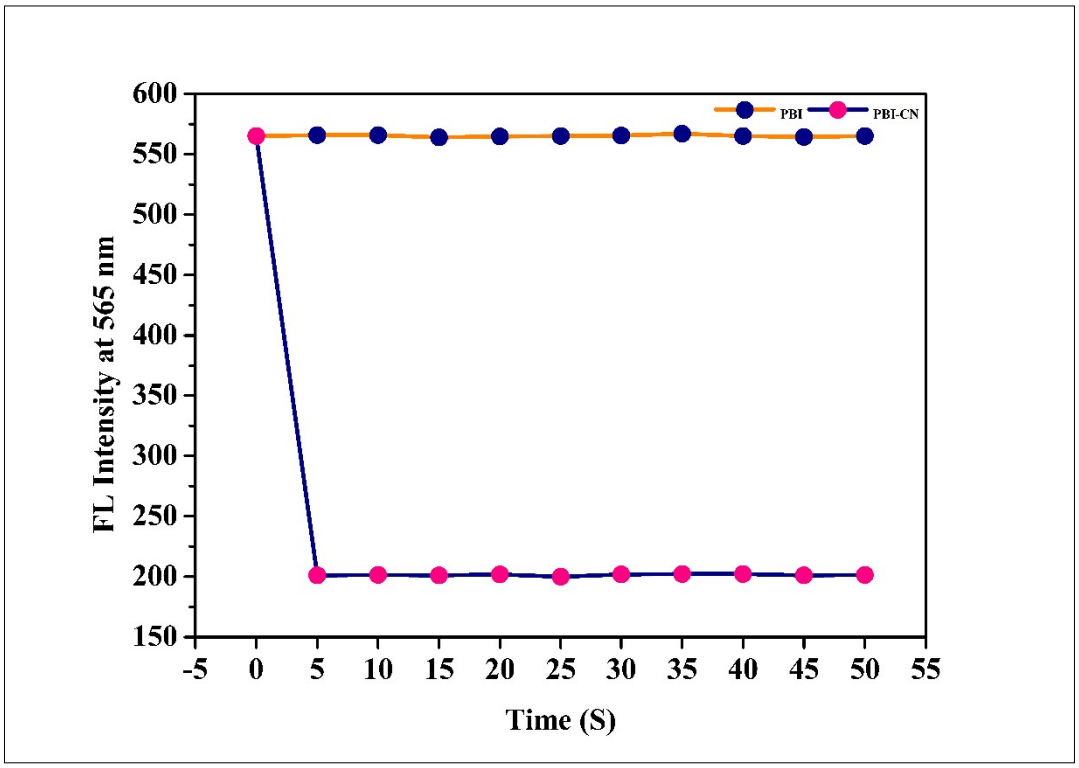

Figure: S11. Time response **PBI** and **PBI**-CN

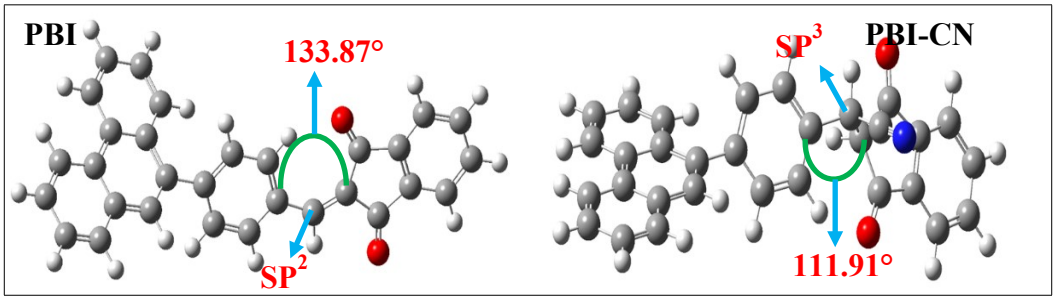

Figure: S12. Ground state optimized structure of **PBI** and **PBI** -CN

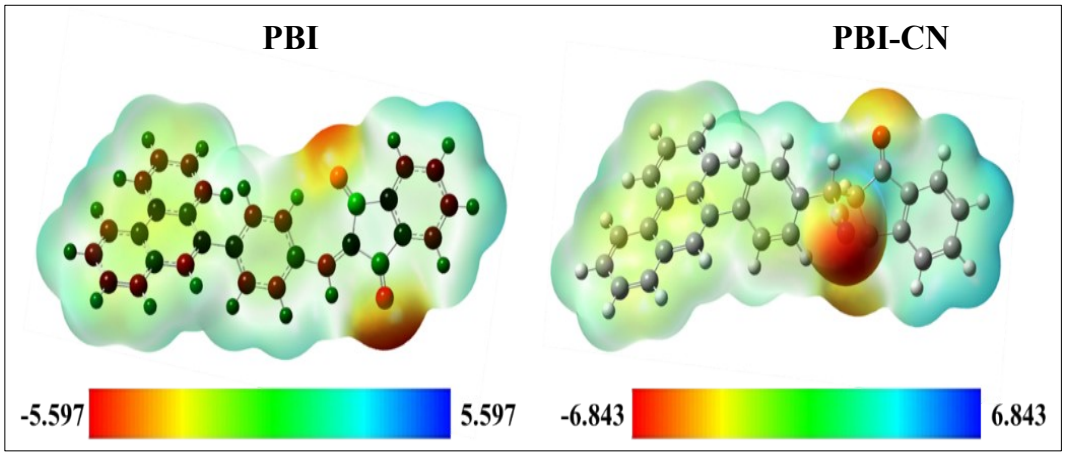

Figure: S13. Molecular electrostatic potential map (MEP)

Table: S4 Fluorescence Lifetime Parameters of compound **PBI** and **PBI**-CN

System	λ_{ex} (nm)	λ_{em} (nm)	τ_1(ns) (Rel %)	τ_2 (ns) (Rel %)	τ_3 (ns) (Rel %)	τ Average (ns)	χ^2
PBI	430	565	0.11	6.23	0.11	0.12	1.15
PBI-CN	440	565	1.82	6.16	0.09	5.27	1.06

Sample	Added (μ mol L^{-1})	Detected (μ mol L^{-1})	Recovery (n=3, %)	RSD (n=3, %)
sprouted potatoes	20	19.98	99.93	1.24
bitter almonds	20	19.87	99.35	0.95
cassava tubers	20	19.99	99.95	3.00
apple seeds	20	19.99	99.95	10.85

Table: S5. Analytical Performance of the Proposed Method for food Samples

Table: S6. Analytical Performance of the Proposed Method for Water Samples

Sample	Added (μ mol L^{-1})	Detected (μ mol L^{-1})	Recovery (n=3, %)	RSD (n=3, %)
Madurai Groundwater Tamil Nadu, India	2	2.0047	100.23	3.40
	4	4.0047	100.11	2.70
	6	6.0015	100.02	2.18

Thamirabarani river water. Tamil Nadu, India.	2 4 6	2.0015 4.0015 6.0015	100.07 100.03 100.02	2.31 4.09 1.29
Ramnad seawater Tamil Nadu, India	2 4 6	2.0015 4.0047 5.9984	100.07 100.11 99.97	0.34 0.94 1.13

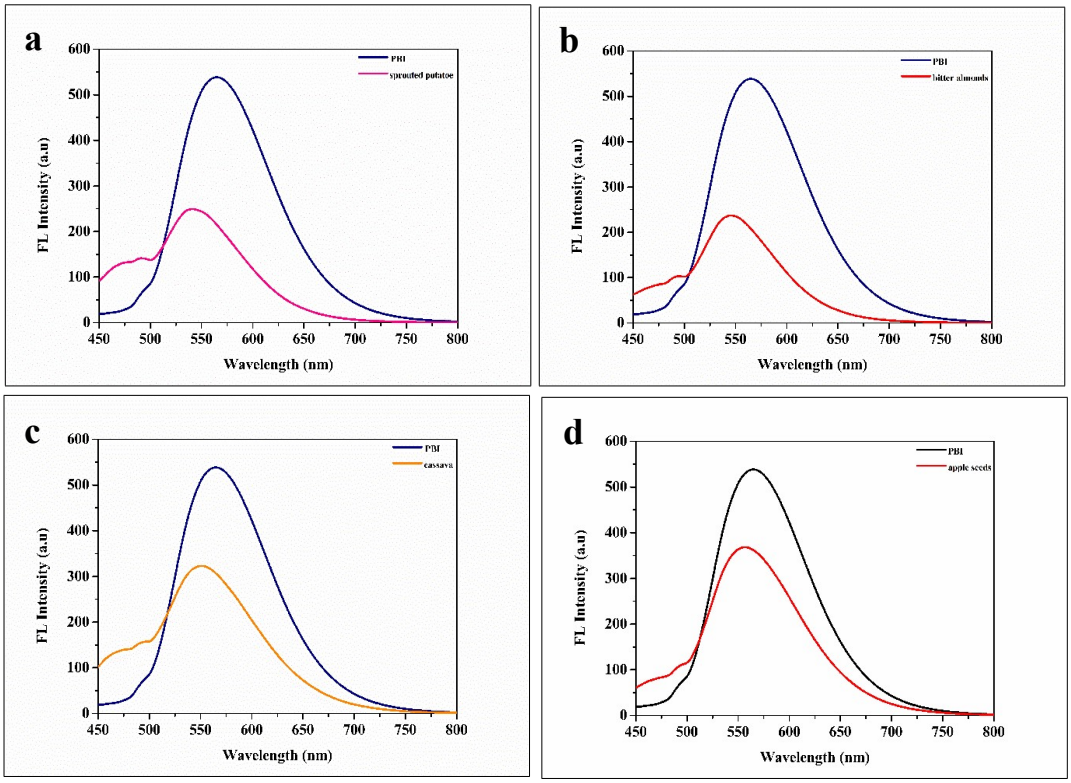

Figure: S14. The fluorescence spectra of PBI in the presence of cyanide-containing extracts from (a) sprouted potatoes, (b) bitter almonds, (c) cassava tubers, and (d) apple seeds.

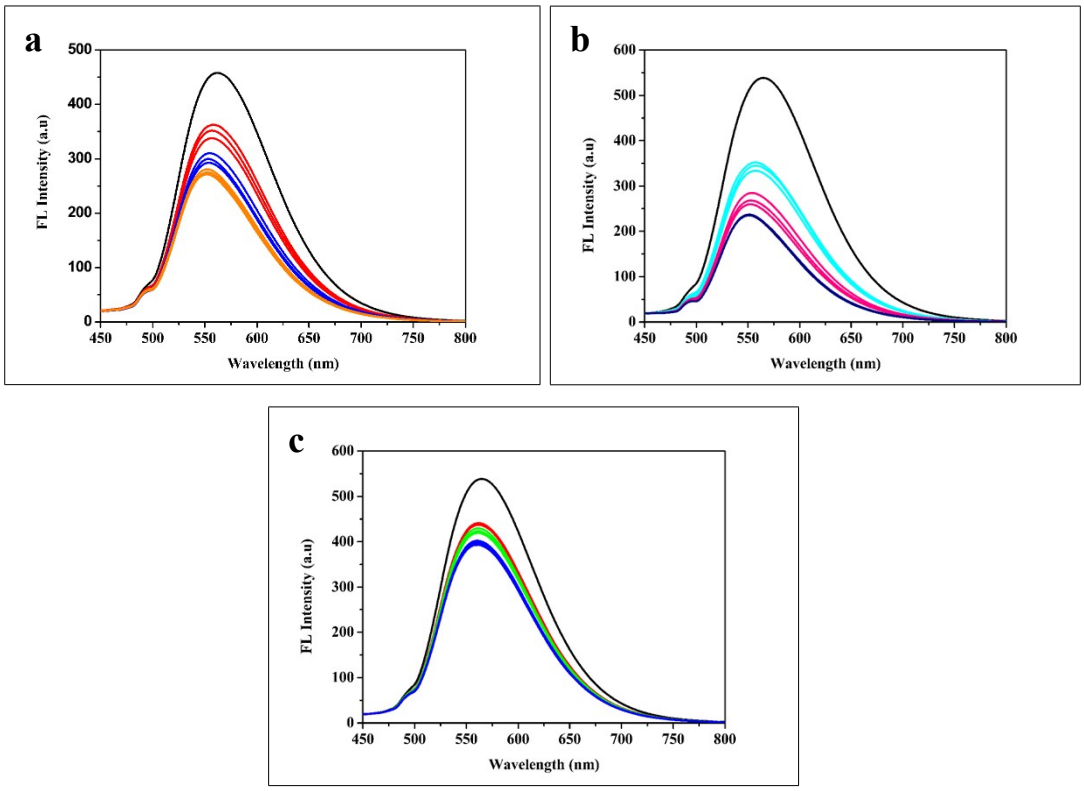

Figure: S15. Emission spectra of probe **PBI** were recorded in the presence of varying concentrations of real water samples, including (a) Madurai groundwater, (b) Thamirabarani river water, and (c) Ramnad seawater (Tamil Nadu, India) in DMSO solvent system.

PBI (µg/ mL)	Cell viability (%)	SD
Control	100	4.27
20	78.52	4.33
40	55.61	5.84
60	48.26	9.77
80	37.47	7.20
100	35.90	1.10

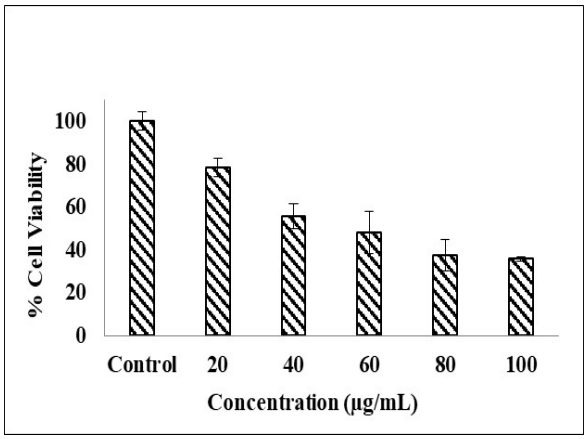

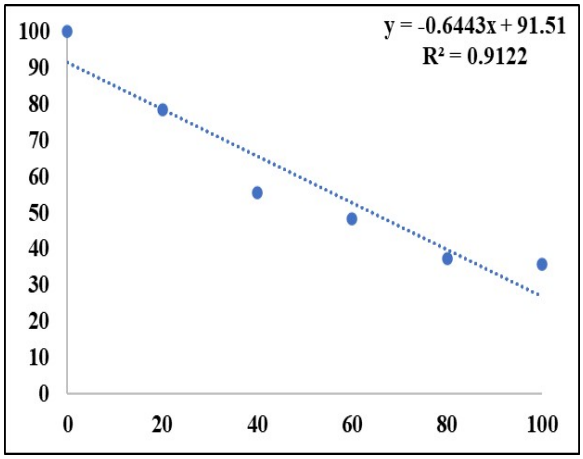

Figure: S16 MTT assay of **PBI** on HEK293T Cell line (24 h)

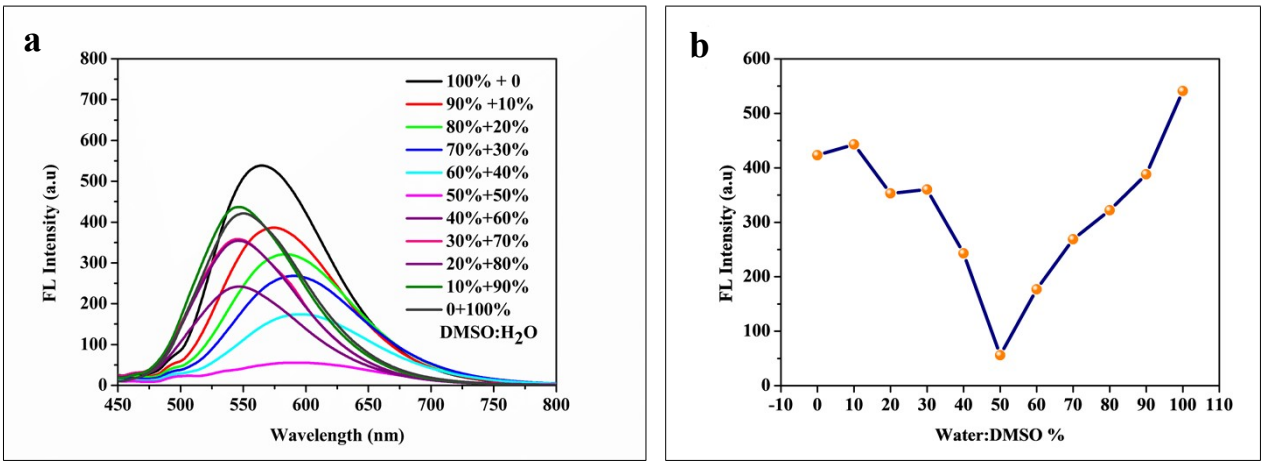

Figure: S17 (a) Emission spectrum of PBI various ratio of DMSO: H_2O (b) Various Ratios of DMSO and Water

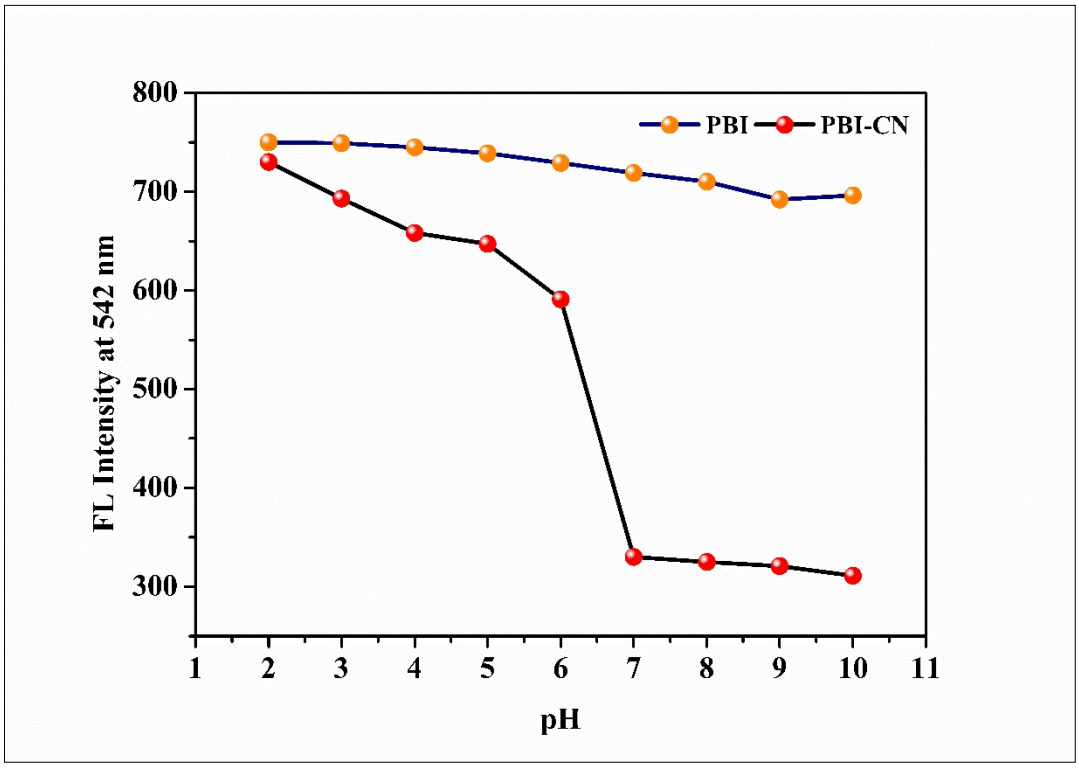

Figure: S18 pH study of PBI and PBI-CN

Reference

S1 S. Huanhuan, D. Weiwei, L. Chunxia, L. Zhanxian, Z. Hongyan, W. Liuhe, Y. Mingming, *Sensors and Actuators B: Chemical*, 2018, **273**, 927-934.

S2 S. Alam, A.S. Sohail, Y.A.A. Abdullah, Zulfiqar Ali Khan, Y. Muhammad, R. Waqar, *Spectro.chim. Acta Part A: Molecular and Biomolecular Spectroscopy* 2025, **327**, 125414.

S3 O. Mehmet, E Serkan, M. Sait, *Analytica Chimica Acta*, 2022, **1227**, 340320.

S4 Z. Fang, Z. Rong, L. Xiaozhong, G. Kunpeng, H. Zhaoxiang, L. Xiaoqing, X. Jingjuan, L. Jie, L. Da, T. Xia, *Dyes and Pigments*, 2018, **155**, 225–232.

S5 T. Jiaqi, W. Yijia, M. Ju, W. Jian, Q. Anjun, Z.S. Jing, Z.T. Ben, *Chemistry A European journal*, 2014, **16** (20), 4661-4670.